Journal of Nuclear Medicine, published on March 14, 2024 as doi:10.2967/jnumed.123.267075

Strong Correlation Between SUV_{max} on PSMA PET/CT and Numeric Drop-In γ-Probe Signal for Intraoperative Identification of Prostate Cancer Lesions

Anne-Claire Berrens*[1,2], Malou A. Sorbi*[1], Maarten L. Donswijk[3], Hilda A. de Barros[1], Samaneh Azargoshasb[1,2], Matthias N. van Oosterom[1,2], Daphne D.D. Rietbergen[1,2,4], Elise M. Bekers[5], Henk G. van der Poel[1,6], Fijs W.B. van Leeuwen[1,2], and Pim J. van Leeuwen[1]

[1]*Department of Urology, Netherlands Cancer Institute–Antoni van Leeuwenhoek Hospital, Amsterdam, The Netherlands;* [2]*Interventional Molecular Imaging Laboratory, Department of Radiology, Leiden University Medical Centre, Leiden, The Netherlands;* [3]*Department of Nuclear Medicine, Netherlands Cancer Institute–Antoni van Leeuwenhoek Hospital, Amsterdam, The Netherlands;* [4]*Department of Nuclear Medicine, Leiden University Medical Centre, Leiden, The Netherlands;* [5]*Department of Pathology, Netherlands Cancer Institute–Antoni van Leeuwenhoek Hospital, Amsterdam, The Netherlands; and* [6]*Department of Urology, Amsterdam University Medical Centre, Location VUmc, Amsterdam, The Netherlands*

Prostate-specific membrane antigen (PSMA) PET is used to select patients with recurrent prostate cancer for metastasis-directed therapy. A surgical approach can be achieved through radioguided surgery (RGS), using a Drop-In γ-probe that traces lesions that accumulate the radioactive signal. With the aim of guiding patient selection for salvage surgery, we studied the correlation between the SUV_{max} of lesions on preoperative PSMA PET/CT and their intraoperative counts/s measured using the Drop-In γ-probe. **Methods:** A secondary analysis based on the prospective, single-arm, and single-center feasibility study was conducted (NCT03857113). Patients ($n = 29$) with biochemical recurrence after previous curative-intent therapy and a maximum of 3 suggestive lesions within the pelvis on preoperative PSMA PET/CT were included. Patients treated with androgen deprivation therapy within 6 mo before surgery were excluded. All patients received an intravenous injection of ^{99m}Tc-PSMA-I&S 1 d before surgery. Radioguidance was achieved using a Drop-In γ-probe. Correlation was determined using the Spearman rank correlation coefficient (ρs). Subgroup analysis was based on the median SUV_{max}. **Results:** In total, 33 lesions were visible on the PSMA PET/CT images, with a median overall SUV_{max} of 6.2 (interquartile range [IQR], 4.2–9.7). RGS facilitated removal of 31 lesions. The median Drop-In counts/s were 134 (IQR, 81–220) in vivo and 109 (IQR, 72–219) ex vivo. The intensity of the values correlated with SUV_{max} (ρs = 0.728 and 0.763, respectively; $P < 0.001$). Subgroup analysis based on median SUV_{max} in the group with an SUV_{max} of less than 6 showed no statistically significant correlation with the numeric signal in vivo (ρs = 0.382; $P = 0.221$) or the signal-to-background-ratio (ρs = 0.245; $P = 0.442$), whereas the group with an SUV_{max} of 6 or more showed respective statistically significant positive correlations (ρs = 0.774 [$P < 0.001$] and ρs = 0.647 [$P = 0.007$]). **Conclusion:** Our findings indicate that there is a direct relation between SUV_{max} on PSMA PET/CT and the readout recorded by the surgical Drop-In probe, thereby indicating that SUV_{max} can be used to select patients for PSMA RGS. For more definitive subgroup definitions for treatment recommendations, further studies are necessary to validate the present findings.

Key Words: SUV_{max}; radioguided surgery; prostate specific membrane antigen; PSMA PET/CT; prostate cancer; γ-probe

J Nucl Med 2024; 00:1–7
DOI: 10.2967/jnumed.123.267075

Despite curative-intent treatment in primary prostate cancer, recurrences occur in 20%–40% of patients (*1*,*2*). Targeting the prostate-specific membrane antigen (PSMA), a protein that is highly overexpressed on the surface of most prostate cancer cells, supports PET imaging. A technology that has substantially enhanced the diagnosis of prostate cancer metastases in intermediate- and high-risk primary patients (*3*), PSMA PET/CT can detect metastatic lesions in patients with biochemical recurrence at prostate-specific antigen (PSA) values of less than 0.5 ng/mL (*4*,*5*), thereby enabling curative metastasis-directed treatment options such as salvage radiotherapy and salvage lymph node dissection.

To accommodate PSMA-targeted surgery, γ-emitting PSMA ligands have been developed that facilitate image-guided surgery (*6*,*7*). In a PSMA-guided workflow, PSMA PET/CT provides the surgical road map, and a secondary PSMA ligand is used to provide intraoperative guidance. Signal intensities of primary tumors on PSMA PET/CT (SUV_{max}) have been reported to vary substantially (*8*).

For guidance during surgery, the γ-emitting ^{99m}Tc-based tracer [^{99m}Tc]Tc-PSMA-I&S has been most frequently used (*9*). This agent not only facilitates PSMA ligand SPECT/CT, albeit with an inferior performance compared with PSMA PET/CT (*10*,*11*), but also facilitates intraoperative lesion localization via γ-tracing (counts/s) (*12*), so-called radioguided surgery (RGS) (Fig. 1). Expanding from traditional γ-probes in open surgery (*12–15*), the introduction of the miniaturized Drop-In γ-probe (Eurorad S.A.) facilitated dissemination of these procedures to robotic surgery (*16–19*). Limited research has been conducted on the SUV_{max} in relation to intraoperative numeric signal. Although the intraoperative counts/s vary substantially (*18*,*19*), there are indications that these values relate to the SUV_{max} (*20*).

The aim of this study was to further corroborate the relation between the SUV_{max} on PSMA PET/CT and the surgical signal

Received Nov. 16, 2023; revision accepted Jan. 11, 2024.
For correspondence or reprints, contact Anne-Claire Berrens (a.berrens@nki.nl).
*Contributed equally to this work.
Published online Mar. 14, 2024.

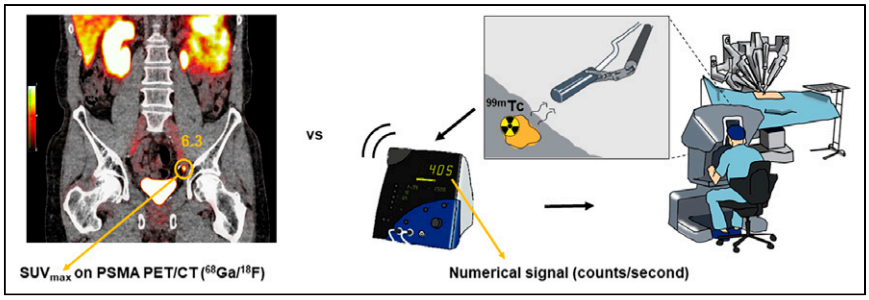

FIGURE 1. Illustration of PSMA PET/CT vs. numeric signal (counts/s) as seen by operating surgeon during robot-assisted surgery.

detected using [^{99m}Tc]Tc-PSMA-I&S. Ultimately, the goal is to identify cutoffs that can be used to refine the selection criteria for PSMA-targeted RGS.

MATERIALS AND METHODS

Study Design and Patient Population

A secondary analysis was performed on data from a prospective, single-center feasibility study that was approved by the local ethics committee at The Netherlands Cancer Institute (ClinicalTrials.gov identifier NCT03857113). All subjects gave written informed consent. The institutional review board approved this retrospective study (IRBdm21-106). Patients were included if they had biochemical recurrence (PSA between 0.2 and 4 ng/mL at 2 consecutive measurements) after previous curative-intent treatment and a maximum of 3 soft-tissue lesions (local or nodal recurrences) on PSMA PET/CT. Patients were excluded if they were receiving androgen deprivation therapy within 6 mo prior to surgery. Patients were treated with robot-assisted ^{99m}Tc-PSMA–targeted salvage RGS between June 2020 and November 2022 (*19*).

Preoperative Imaging and Analysis

All patients underwent PSMA PET/CT within the Prostate Cancer Network Netherlands (*Prostaatkankernetwerk Nederland*). Patients were scanned using [^{68}Ga]Ga-PSMA-11, [^{18}F]DCFPyl, or [^{18}F]JK-PSMA-7 within 125 d before RGS, according to local protocols. Two experienced nuclear medicine physicians reevaluated the preoperative imaging using Osirix MD (Pixmeo SARL). On preoperative PSMA PET/CT, the SUV_{max} of lesions noted in the clinical report was determined by drawing a volume of interest over the lesions. The short-axis diameter of the morphologic substrate, if visible on concurrent CT, was measured.

One day before surgery, a single dose of [^{99m}Tc]Tc-PSMA-I&S (median, 541 MBq; interquartile range [IQR], 482–559 MBq) was injected intravenously and assessed by performing SPECT/CT on the morning of surgery, a median of 17 h (IQR, 17.3–17.8 h) after the injection. The preoperative scintigraphy was reevaluated after the evaluators had been masked to clinical or study-related data, including the preoperative PSMA PET/CT and intraoperative findings. The number and location of suggestive lesions were noted.

Intraoperative Measurements

Within a median of 21 h after injection, RGS was performed. All surgical procedures were done using a da Vinci Xi robot (Intuitive Surgical). Radioguidance was achieved using a Drop-In γ-probe translating the radiosignal to the numeric signal. First, radiotracer activity measurements of anatomic landmarks near target prostate cancer lesions (i.e., iliac artery, iliac vein, and psoas muscle) were performed to determine the background signal. Second, the locations of the suspected prostate cancer lesions were scanned in vivo with the Drop-In probe to assess the signal-to-background ratio (SBR). To confirm successful removal of radioactive tissue, ex vivo validations were performed using the Drop-In γ-probe. A detailed description of the surgical procedures was provided by de Barros et al. (*19*).

Histopathologic Evaluation and Immunohistochemistry

All dissected specimens were sent for histopathologic examination with hematoxylin and eosin staining and, if needed, immunohistochemical pan cytokeratin AE13 (cytokeratin AE1 and AE3) staining. On prostate cancer–positive tissues, additional immunohistochemical PSMA staining was performed (clone 3E6; Dako) to assess the PSMA intensity. The total immunostaining score (TIS) was calculated using:

$$\text{TIS} = \text{proportion score} \times \text{corresponding intensity scores}.$$

The proportion score represented the percentage of cells that stained positively with a particular intensity and could range between 0% and 100%. The intensity score represented the intensity of the stained cells and could range between 0 and 3 (0, no staining; 1, weak; 2, moderate; 3, strong). One pathologist analyzed all intraoperative obtained tissues. The size of the node was measured along the long axis. The TIS of each tumor-positive region was correlated with the SUV_{max} and the numeric signal of the in vivo and ex vivo measurements.

Statistical Analysis

Data were summarized by frequency and percentage for categoric variables and mean and median with ranges for continuous variables. The numeric signal was normalized to account for differences in injected activity of ^{99m}Tc, using the average injected dose as the standard (550 MBq). For continuous variables, normality of distribution was verified with Kolmogorov–Smirnov testing. The primary outcome of interest was the correlation of the SUV_{max} of the prostate cancer lesions on preoperative PSMA PET/CT and the in vivo numeric signal of the PSMA-positive prostate cancer lesions recorded with the Drop-In γ-probe. A secondary outcome was the ex vivo signal and the PSMA intensity on histopathology's correlation with SUV_{max}. All were analyzed using the Spearman rank correlation coefficient (ρs) to determine the correlation. To evaluate the visual perception of a potential correlation, a scatterplot was produced. The different PSMA PET tracers were compared using a Kruskal–Wallis statistical test, and the SPECT/CT subgroups were compared using a Mann–Whitney *U* statistical test. To identify meaningful subgroups for clinical applicability, median regression with concave fusion penalizations was used (*21*). A *P* value of less than 0.05 was considered statistically significant. Statistical analysis was performed with SPSS Statistics, version 29.0 (IBM).

RESULTS

Patient Characteristics

After staging on PSMA PET/CT, 29 patients who had suspected nodal disease ($n = 25$) or locally recurrent prostate cancer ($n = 4$) were included (Fig. 2). As primary treatment, 21 patients (72%) underwent radical prostatectomy and 8 (28%) underwent radiotherapy. Subsequently, 13 patients (45%) underwent salvage therapy before [^{99m}Tc]Tc-PSMA RGS (Table 1).

Preoperative Imaging and Analysis

In total, 33 PSMA-avid lesions were identified on the preoperative PSMA PET/CT. The overall median SUV_{max} on preoperative PSMA PET/CT was 6.2 (IQR, 4.2–9.7) and did not differ between

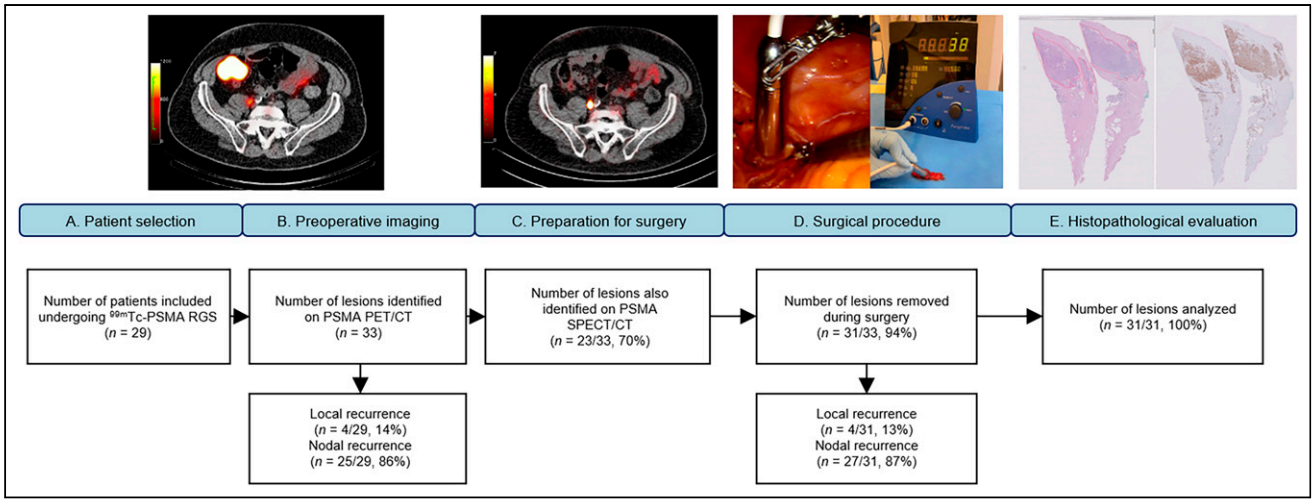

FIGURE 2. Workflow and inclusions. (A–C) Patient selection for salvage [^{99m}Tc]Tc-PSMA RGS (A), preoperative PSMA PET/CT (B), and [^{99m}Tc]Tc-PSMA-I&S imaging (C) demonstrate parailiac lesion in patient with biochemical recurrence. (D) Intraoperative activity measurements with Drop-In γ-probe. (E) Immunohistochemistry (PSMA staining) at histopathologic examination.

TABLE 1
Patient Characteristics

Parameter	Result
Age at [^{99m}Tc]Tc-PSMA RGS (y)	68 (66–72)
Previous primary treatment	
RALP	4 (14)
RALP + ePLND	17 (59)
EBRT	2 (7)
EBRT + HT	5 (17)
Brachytherapy	1 (3)
Previous salvage treatment	
Radiotherapy fossa	5 (17)
Radiotherapy prostate + pelvis	3 (10)
Salvage prostatectomy + LND	1 (3)
Radiotherapy pelvis	1 (3)
Radiotherapy fossa + SLND	1 (3)
Radiotherapy fossa + lutetium PSMA	1 (3)
Radiotherapy prostate + pelvis + previous SLND	1 (3)
No previous salvage treatment	16 (55)
Type of recurrence	
Nodal	25 (86)
Local	4 (14)
PSA before [^{99m}Tc]Tc-PSMA RGS	0.91 (0.5–2.4)
Number of positive lesions on PSMA PET/CT	
1 lesion	25 (86)
2 lesions	4 (14)

RALP = robot-assisted laparoscopic prostatectomy; ePLND = extended pelvic lymph node dissection; EBRT = external-beam radiation therapy; HT = hormone therapy; (S)LND = (salvage) lymph node dissection.

Qualitative data are number and percentage; continuous data are median and IQR.

the different tracers ($P = 0.559$) (Table 2). Ninety-seven percent of the PSMA PET/CT scans were conducted on a European Association of Nuclear Medicine Research Ltd.–accredited system (*22*,*23*). Twenty-seven of the 33 (82%) identified lesions were smaller than 1 cm, with a median size of 4 mm (IQR, 3.8–6 mm). The size of the PSMA PET/CT–avid lesion correlated significantly with the SUV_{max} ($\rho s = 0.728$; $P < 0.001$). The PSA before RGS showed a weak, nonsignificant correlation with the SUV_{max} ($\rho s = 0.2041$; $P = 0.289$), as did the PSA density (defined as PSA before surgery multiplied by the size of the lesion or lesions on PSMA PET/CT) ($\rho s = 0.390$; $P = 0.073$).

Of the 33 lesions found on PSMA PET/CT, 23 (70%) were observed on PSMA-I&S SPECT/CT and 10 (30%) were not. Within the group of lesions that were not visible on SPECT/CT, the median SUV_{max} was 4.9 (IQR, 3.3–6.4), whereas the group of lesions visible on SPECT/CT had a median SUV_{max} of 7.4 (IQR, 5.3–14.3) ($P = 0.028$). Visibility on SPECT/CT was not associated with a higher numeric signal in vivo ($P = 0.237$) or a higher SBR ($P = 0.453$)

Intraoperative

In total, 31 of 33 (94%) lesions were successfully removed during robot-assisted RGS. One suggestive LN could not be localized because of extensive intestinal adhesions (3 mm on PSMA PET/CT; SUV_{max}, 5.3), and 1 LN (3 mm on PSMA PET/CT; SUV_{max}, 1.8) located in the pararectal fat could not be detected because of high

TABLE 2
Characteristics of Diagnostic Preoperative Imaging and Preparation for Surgery

Parameter	Result
Diagnostic preoperative imaging	
Type of PSMA PET/CT	
[^{68}Ga]Ga-PSMA	6 (21)
[^{18}F]DCFPyL	13 (45)
[^{18}F]JK-PSMA-7	10 (34)
Median incubation time (min)	58 (50–61)
[^{68}Ga]Ga-PSMA	49 (44–52)
[^{18}F]DCFPyL	58 (56–61)
[^{18}F]JK-PSMA-7	61 (58–74)
Dose of PSMA PET/CT tracer (MBq)	197 (161–201)
[^{68}Ga]Ga-PSMA	146 (134–159)
[^{18}F]DCFPyL	180 (164–203)
[^{18}F]JK-PSMA-7	201 (200–202)
SUV_{max} of suspected lesion on PSMA PET/CT overall	6.2 (4.2–9.7)
[^{68}Ga]Ga-PSMA	7.7 (3.0–11.6)
[^{18}F]DCFPyL	5.5 (4.2–9.1)
[^{18}F]JK-PSMA-7	6.4 (4.8–16.2)
Time from PSMA PET/CT to operation (d)	33 (15–50)
Size of suspected lesion on PSMA PET/CT (mm)	4 (3.8–6)
Size of suspected lesion on PSMA PET/CT	
<1 cm	27 (82)
≥1 cm	4 (12)
Not measurable	2 (6)
EARL accreditation for PSMA PET/CT	
Yes	28 (97)
No	1 (3)
Preparation for surgery	
Dose of ^{99m}Tc-tracer (MBq)	541 (482–559)
Time from injection of ^{99m}Tc-tracer to SPECT/CT (h)	17.25 (17.25–17.75)
Lesion visible on PSMA PET/CT also visible on SPECT/CT	
Yes	23 (70)
No	10 (30)

EARL = European Association of Nuclear Medicine Research Ltd.
Qualitative data are number and percentage; continuous data are median and IQR.

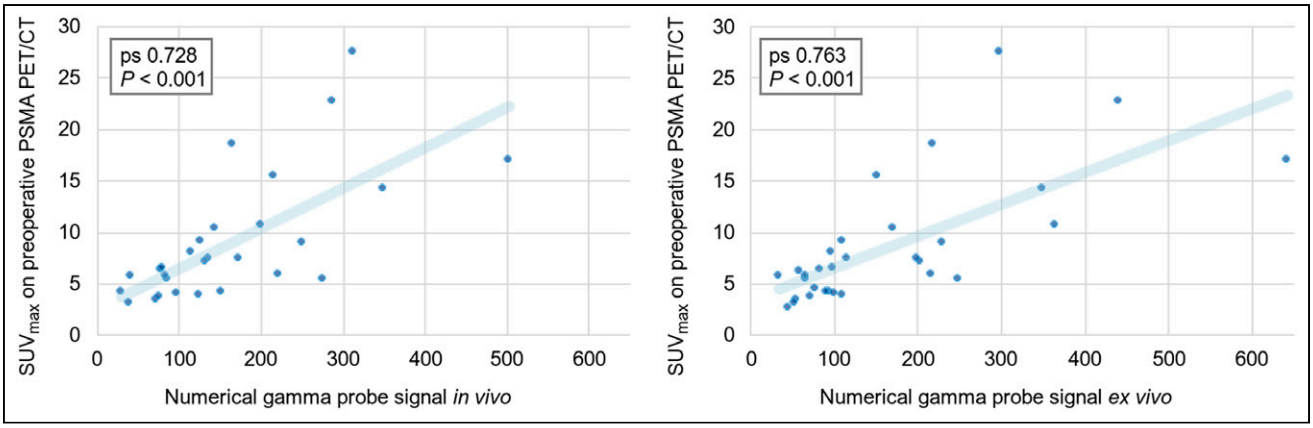

FIGURE 3. Scatterplot illustrating correlation between SUV_{max} on preoperative PSMA PET/CT and in vivo and ex vivo numeric signal of Drop-In γ-probe.

background signal in the rectum as a result of hepatobiliary tracer clearance. The numeric signal of the lesion was recorded both in vivo and ex vivo (median, 134 counts/s [IQR, 81–220] and 109 counts/s [IQR, 72–219], respectively). The median SBR in vivo was 2.3 (IQR, 1.7–3.9). No correlation was seen between the duration of the surgery (median, 136 min; IQR, 101–155) and the SUV_{max} (ρs = −1.44; $P = 0.457$) or the counts in vivo (ρs = −1.38; $P = 0.492$).

Correlation Between SUV_{max} and Intraoperative Numeric Signal

A significant and strong positive correlation was found between the overall SUV_{max} and the intraoperative measures (ρs = 0.728 and 0.763 for in vivo and ex vivo, respectively; $P < 0.001$) (Fig. 3). Median regression analysis identified 2 SUV_{max} subgroups (<6 and ≥6). The former subgroup showed no statistically significant correlation with the numeric signal in vivo (ρs = 0.382; $P = 0.221$), whereas the latter did (ρs = 0.774; $P < 0.001$). Ex vivo results were similar ($SUV_{max} < 6$, ρs = 0.308 [$P = 0.284$]; $SUV_{max} \geq 6$, ρs = 0.752 [$P < 0.001$]). A very moderate, nonsignificant, correlation was observed between the size of the lesion on preoperative PSMA PET/CT and numeric signal in vivo (ρs = 0.421; $P = 0.057$) and ex vivo (ρs = 0.492; $P = 0.015$).

Overall, a moderate correlation was found for the SUV_{max} of the prostate cancer lesions on preoperative PSMA PET/CT and the SBR in vivo (ρs = 0.524; $P = 0.004$). Subgroup analysis showed no correlation between an SUV_{max} of less than 6 (ρs = 0.245; $P = 0.442$) and the SBR, whereas a strong correlation was observed for lesions with an SUV_{max} of 6 or higher (ρs = 0.647; $P = 0.007$).

Correlation Between SUV_{max} and PSMA Intensity Staining

Among the removed lesions, the median TIS was 2.3 (IQR, 2.0–3.0) (Table 3). The distribution of PSMA intensity was homogeneous in 46% of the lesions and heterogeneous in 54%. The type of distribution had no significant impact on SUV_{max} ($P = 0.602$). No positive correlation was found between SUV_{max} and TIS (ρs = −0.433; $P = 0.015$). Multiplying TIS by the size of the lesion at pathology did not show a correlation with SUV_{max} on preoperative PSMA PET/CT (ρs = 0.190; $P = 0.353$).

DISCUSSION

By directly comparing pre- and intraoperative PSMA-targeting strategies, we could identify a significant, positive correlation between SUV_{max} and Drop-In γ-probe measurements. The higher the SUV_{max} is, the greater is the distinction between the tumor and surrounding structures in vivo, suggesting a more reliable road map. Lesion identification may seem less straightforward with a lower SUV_{max} but was not impossible since nearly all lesions in the present study were identified and removed. Our results are in line with the findings of Gondoputro et al., who performed successful RGS on lesions with a median SUV_{max} of 4.4 (*18*). SUV_{max} should therefore be considered among various parameters in the case assessment. Not all removed lesions were seen on the preoperative SPECT/CT, possibly because of timing and background interference (*11*). Although one might assume that the greater the distinction the shorter the duration of the surgery, the current results are inconclusive in this regard. A possible explanation might be the other factors that influence duration, such as adhesions, the type of tissue surrounding the lesion, and the learning curve of the operating surgeon.

On the basis of median regression, we defined 2 SUV_{max} subgroups (<6 and ≥6) that showed clear differences in sensitivity and specificity. However, external validation of these findings is needed in larger series since subgroups were not defined a priori. Nevertheless, with an increasing population subjected to

TABLE 3
Intraoperative and Histopathologic Outcomes

Parameter	Result
Intraoperative outcome	
Time from injection of ^{99m}Tc-tracer to operation (h)	21 (19.75–21.1)
Lesions removed during operation	31 (94)
Counts/s Drop-In γ-probe in vivo	134 (81–220)
Counts/s Drop-In γ-probe ex vivo	109 (72–219)
Counts/s in suspected lesion to activity in PAV ratio (SBR)	2.3 (1.7–3.9)
Histopathologic outcome, TIS	2.3 (2.0–3.0)

PAV = psoas, artery, and vein; TIS = total immunostaining score; SBR = signal-to-background ratio.

Qualitative data are number and percentage; continuous data are median and IQR.

oligometastatic treatment by PSMA RGS (*9*), definitions of optimal subgroups for RGS are desired.

For clinical applicability it would be less time-consuming to base the preoperative assessment on the size of the lesion. This study showed, however, that lesion size was not a significant predictor for the number of intraoperative numeric signal, whereas SUV_{max} appeared to be a strong and significant predictor and should therefore be preferred when selecting patients.

No positive correlation was observed between SUV_{max} and PSMA intensity staining defined as the TIS, possibly because of the wide variation in SUV_{max} and the fact that TIS ranged mostly from moderate to strong. Another influential factor could be the reporting of lymph node size solely as diameter, and the evaluation of TIS per slide, which omits consideration of its 3 dimensions. Little is known regarding the TIS and SUV_{max} of prostate cancer–positive lymph nodes. Looking at radical prostatectomy specimens, Rüschoff et al. also found no significant correlation between SUV_{max} on PSMA PET/CT and immunohistochemical PSMA intensity expression (*24*), whereas Jiao et al. and Vetrone et al. did find a correlation (*25*,*26*), possibly explained by different tumor characteristics or growth patterns (*8*).

Limitations include the high variability in a relatively small number of included patients and the retrospective nature of the secondary analysis. For the scope of this article, only PSMA PET/CT–positive nodes were included. The inclusion criteria of the prospective study introduce a possible selection bias (*19*). The nature of the surrounding tissue is always a consideration when measuring activity in vivo. To minimize the effect of background signal, in the prospective study the values were documented in real time after careful positioning of the Drop-In γ-probe. A limitation remains, however, in that the surrounding tissue type was not considered in this secondary analysis. In addition, applicability in open surgery was not studied.

Subgroup analysis was performed although subgroups were not specified a priori; inferential issues might therefore emerge. Subgroups based on the median are dependent on the cohort and may alter slightly after validation in larger cohorts. Furthermore, there were differences in the median SUV_{max} used for different PSMA PET/CT tracers and systems—although an accurate representation of daily clinical practice. Although our groups were much smaller, the differences were similar to those seen by de Bie et al., who found recurrent prostate cancer to have a nonsignificantly higher SUV_{max} in the [^{68}Ga]Ga-PSMA-11 group (*27*). In addition, all surgical procedures were performed in a single tertiary center experienced in the use of ^{99m}Tc-tracers and the Drop-In γ-probe.

With the growing implementation of PSMA RGS and minimally invasive robotic surgery, it is expected that PSMA PET/CT will assume a fundamental role in the selection of patients, thereby helping to optimize the treatment of patients with oligometastatic prostate cancer recurrence and perhaps also during primary treatment.

CONCLUSION

This study showed a significant positive correlation between the SUV_{max} on preoperative PSMA PET/CT and the intraoperative numeric signal measured by the Drop-In γ-probe, thereby indicating that SUV_{max} can be considered a parameter to select patients for PSMA RGS. Further studies are needed to validate the present subgroup definitions before treatment recommendations can be made.

DISCLOSURE

Fijs W.B van Leeuwen is supported by an NWO-TTW-VICI grant (TTW 16141). No other potential conflict of interest relevant to this article was reported.

KEY POINTS

QUESTION: Does the SUV_{max} on preoperative PSMA PET/CT correlate with the intraoperative γ-probe signal during radioguided prostate cancer surgery?

PERTINENT FINDINGS: A secondary analysis based on the prospective, single-arm, and single-center feasibility study was conducted. Results showed a strong and statistically significant correlation between the SUV_{max} on preoperative PSMA PET/CT and the intraoperative numeric γ-probe signal

IMPLICATIONS FOR PATIENT CARE: Our findings of a direct relation between the SUV_{max} on PSMA PET/CT and the intraoperative signal indicates that SUV_{max} can be considered among other parameters to select patients for PSMA RGS.

ACKNOWLEDGMENTS

We thank the nuclear medicine, pathologic, and surgical staff of the Netherlands Cancer Institute.

REFERENCES

1. Boorjian SA, Houston Thompson R, Tollefson MK, Rangel LJ, Bergstralh EJ, Blute ML. Long-term risk of clinical progression after biochemical recurrence following radical prostatectomy: the impact of time from surgery to recurrence. *Eur Urol.* 2011;59:893–899.
2. Suardi N, Porter CR, Reuther AM, et al. A nomogram predicting long-term biochemical recurrence after radical prostatectomy. *Cancer.* 2008;112:1254–1263.
3. Hofman MS, Lawrentschuk N, Francis RJ, et al. Prostate-specific membrane antigen PET-CT in patients with high-risk prostate cancer before curative-intent surgery or radiotherapy (proPSMA): a prospective, randomised, multicentre study. *Lancet.* 2020;395:1208–1216.
4. Morigi JJ, Stricker PD, van Leeuwen PJ, et al. Prospective comparison of ^{18}F-fluoromethylcholine versus ^{68}Ga-PSMA PET/CT in prostate cancer patients who have rising PSA after curative treatment and are being considered for targeted therapy. *J Nucl Med.* 2015;56:1185–1190.
5. Perera M, Papa N, Roberts M, et al. Gallium-68 prostate-specific membrane antigen positron emission tomography in advanced prostate cancer: updated diagnostic utility, sensitivity, specificity, and distribution of prostate-specific membrane antigen-avid lesions—a systematic review and meta-analysis. *Eur Urol.* 2020;77:403–417.
6. Hensbergen AW, van Willigen DM, van Beurden F, et al. Image-guided surgery: are we getting the most out of small-molecule prostate-specific-membrane-antigen-targeted tracers? *Bioconjug Chem.* 2020;31:375–395.
7. Derks YHW, van Lith SAM, Amatdjais-Groenen HIV, et al. Theranostic PSMA ligands with optimized backbones for intraoperative multimodal imaging and photodynamic therapy of prostate cancer. *Eur J Nucl Med Mol Imaging.* 2022;49:2425–2435.
8. Demirci E, Kabasakal L, Sahin OE, et al. Can SUVmax values of Ga-68-PSMA PET/CT scan predict the clinically significant prostate cancer? *Nucl Med Commun.* 2019;40:86–91.
9. Berrens AC, Knipper S, Marra G, et al. State-of-the-art in prostate specific membrane antigen (PSMA)-targeted surgery: a systematic review *Eur Urol Open Science.* 2023;54:43–55.
10. Koehler D, Sauer M, Klutmann S, et al. Feasibility of ^{99m}Tc-MIP-1404 for SPECT/CT imaging and subsequent PSMA-radioguided surgery in early biochemically recurrent prostate cancer: a case series of 9 patients. *J Nucl Med.* 2023;64:59–62.
11. Berliner C, Steinhelfer L, Chantadisai M, et al. Delayed imaging improves lesion detectability in [^{99m}Tc]Tc-PSMA-I&S SPECT/CT in recurrent prostate cancer. *J Nucl Med.* 2023;64:1036–1042.

12. Maurer T, Weirich G, Schottelius M, et al. Prostate-specific membrane antigen-radioguided surgery for metastatic lymph nodes in prostate cancer. *Eur Urol.* 2015; 68:530–534.
13. Robu S, Schottelius M, Eiber M, et al. Preclinical evaluation and first patient application of ^{99m}Tc-PSMA-I&S for SPECT imaging and radioguided surgery in prostate cancer. *J Nucl Med.* 2017;58:235–242.
14. Rauscher I, Duwel C, Wirtz M, et al. Value of ^{111}In-prostate-specific membrane antigen (PSMA)-radioguided surgery for salvage lymphadenectomy in recurrent prostate cancer: correlation with histopathology and clinical follow-up. *BJU Int.* 2017;120:40–47.
15. Kratzik C, Dorudi S, Schatzl M, Sinzinger H. Tc-99m-PSMA imaging allows successful radioguided surgery in recurrent prostate cancer. *Hell J Nucl Med.* 2018;21: 202–204.
16. van Leeuwen FWB, van Oosterom MN, Meershoek P, et al. Minimal-invasive robot-assisted image-guided resection of prostate-specific membrane antigen-positive lymph nodes in recurrent prostate cancer. *Clin Nucl Med.* 2019;44:580–581.
17. Erfani S, Sadeghi R, Aghaee A, Ghorbani H, Roshanravan V. Prostate-specific membrane antigen radioguided surgery for salvage pelvic lymph node dissection in a man with prostate cancer. *Clin Nucl Med.* 2022;47:e174–e176.
18. Gondoputro W, Scheltema MJ, Blazevski A, et al. Robot-assisted prostate-specific membrane antigen-radioguided surgery in primary diagnosed prostate cancer. *J Nucl Med.* 2022;63:1659–1664.
19. de Barros HA, van Oosterom MN, Donswijk ML, et al. Robot-assisted prostate-specific membrane antigen-radioguided salvage surgery in recurrent prostate cancer using a DROP-IN gamma probe: the first prospective feasibility study. *Eur Urol.* 2022;82:97–105.
20. Azargoshasb S, de Barros HA, Rietbergen DDD, et al. Artificial intelligence-supported video analysis as a means to assess the impact of DROP-IN image guidance on robotic surgeons: radioguided sentinel lymph node versus PSMA-targeted prostate cancer surgery. *Adv Intell Syst.* 2023;5:2300192.
21. Zhang Y, Wang HJ, Zh Z. Robust subgroup identification. *Stat Sin.* 2019;29:1873–1889.
22. Werner RA, Hartrampf PE, Fendler WP, et al. Prostate-specific membrane antigen reporting and data system version 2.0. *Eur Urol.* 2023;84:491–502.
23. Aide N, Lasnon C, Veit-Haibach P, Sera T, Sattler B, Boellaard R. EANM/EARL harmonization strategies in PET quantification: from daily practice to multicentre oncological studies. *Eur J Nucl Med Mol Imaging.* 2017;44:17–31.
24. Rüschoff JH, Ferraro DA, Muehlematter UJ, et al. What's behind ^{68}Ga-PSMA-11 uptake in primary prostate cancer PET? Investigation of histopathological parameters and immunohistochemical PSMA expression patterns. *Eur J Nucl Med Mol Imaging.* 2021;48:4042–4053.
25. Jiao J, Kang F, Zhang J, et al. Establishment and prospective validation of an SUV_{max} cutoff value to discriminate clinically significant prostate cancer from benign prostate diseases in patients with suspected prostate cancer by ^{68}Ga-PSMA PET/CT: a real-world study. *Theranostics.* 2021;11:8396–8411.
26. Vetrone L, Mei R, Bianchi L, et al. Histology and PSMA expression on immunohistochemistry in high-risk prostate cancer patients: comparison with ^{68}Ga-PSMA PET/CT features in primary staging. *Cancers (Basel).* 2023;15:1716.
27. de Bie KCC, Veerman H, Bodar YJL, et al. Higher preoperative maximum standardised uptake values (SUV_{max}) are associated with higher biochemical recurrence rates after robot-assisted radical prostatectomy for [^{68}Ga]Ga-PSMA-11 and [^{18}F]DCFPyL positron emission tomography/computed tomography. *Diagnostics (Basel).* 2023;13:2343.